

THE EFFECTS OF THERMAL CONDUCTION ON RADIATIVELY-INEFFICIENT ACCRETION FLOWS

BRYAN M. JOHNSON AND ELIOT QUATAERT

Astronomy Department, 601 Campbell Hall, University of California at Berkeley, Berkeley, CA 94720

Draft version August 1, 2021

ABSTRACT

We quantify the effects of electron thermal conduction on the properties of hot accretion flows, under the assumption of spherical symmetry. Electron heat conduction is important for low accretion rate systems where the electron cooling time is longer than the conduction time of the plasma, such as Sgr A* in the Galactic Center. For accretion flows with density profiles similar to the Bondi solution ($n[r] \propto r^{-3/2}$), we show that heat conduction leads to super-virial temperatures, implying that conduction significantly modifies the dynamics of the accretion flow. We then self-consistently solve for the dynamics of spherical accretion in the presence of saturated conduction and electron heating. We find that the accretion rate onto the central object can be reduced by $\sim 1 - 3$ orders of magnitude relative to the canonical Bondi rate. Electron conduction may thus be an important ingredient in explaining the low radiative efficiencies and low accretion rates inferred from observations of low-luminosity galactic nuclei. The solutions presented in this paper may also describe the nonlinear saturation of the magnetothermal instability in hot accretion flows.

Subject headings: accretion, accretion disks – Galaxy: center

1. INTRODUCTION

The conversion of gravitational binding energy of accreting matter into radiation is thought to account for the high luminosities observed from many compact objects (e.g., AGN; Lynden-Bell 1969). Most of the time, however, systems that appear to harbor compact objects (low luminosity AGN, X-ray binary systems in quiescence) do not radiate at the levels one would expect from simple estimates of the efficiency at which binding energy is converted to radiation. This implies that these systems have low radiative efficiencies and/or low accretion rates, and that the accreting gas may thus retain most of its binding energy in the form of heat. The ultimate energy sink for such hot radiatively inefficient accretion flows (RIAFs) remains an area of active research. The energy may be primarily advected in with the flow (Narayan & Yi 1994), or it may be directed into driving bulk convective motion (Quataert & Gruzinov 2000a; Narayan et al. 2000) or a global outflow (Blandford & Begelman 1999). Numerical simulations favor the latter possibilities (e.g., Igumenshchev & Abramowicz 1999; Stone & Pringle 2001; Hawley & Balbus 2002).

Another possible outlet for the accretion energy is a heat flux due to thermal conduction. In order to maintain a hot accretion flow, the timescale for electrons and protons to exchange energy by Coulomb collisions exceeds the timescale for the plasma to flow into the central black hole (e.g., Rees et al. 1982). Thus the inflowing plasma is collisionless and energy transport by heat conduction may be dynamically important. Direct observational estimates of the electron mean-free path on scales resolved by *Chandra* in nearby galactic nuclei – including our Galactic Center – give values $\sim 0.02 - 1.3$ times the gravitational radius of influence of the central black hole ($\sim 10^5 - 10^6$ Schwarzschild radii). Thus the plasma is relatively collisionless even at large distances from the black hole (Quataert 2004; Tanaka & Menou 2006). Under these conditions, the magnitude of the heat flux is

uncertain and depends on the geometry of the magnetic field and the effective collision rate due to plasma waves and instabilities. It is plausible, however, that thermal conduction will occur at close to its maximal saturated rate, with a heat flux $F \propto \rho v_e^3$, where ρ is the density and v_e the electron thermal speed (Cowie & McKee 1977). This appears to be true in the solar wind (Salem et al. 2003), a well-studied example of a macroscopically collisionless plasma. For non-relativistic electrons, the ratio of the inflow time to the electron conduction time in a hot accretion flow may be as large as $\sim v_e/v_r$ (see equation [1] below), where v_r is the radial flow velocity. For subsonic inflow (with respect to the ions), this ratio is $\gtrsim \sqrt{m_p/m_e} \sim 40$, highlighting the possible importance of conduction in hot accretion flows. In addition, Balbus (2000) has shown that low collisionality conducting plasmas are unstable to convective-like motions in the presence of an outwardly decreasing temperature gradient (the MTI or magnetothermal instability). Although the interplay between the MTI and the magnetorotational instability (MRI) is uncertain, it is plausible that the MTI will lead to a dynamically important heat flux in hot accretion flows.

Any significant heat flux from the inner (hotter) to the outer (colder) parts of an accretion flow can act to reduce the inflow rate. This is true if energy is transported by radiation (e.g., Ostriker et al. 1976), viscous stresses (e.g., Blandford & Begelman 1999), convection (e.g., Quataert & Gruzinov 2000a), or thermal conduction, the focus of this paper. Gas in the outer region of a spherical accretion flow near the sonic point has a thermal energy comparable to its gravitational binding energy. Additional heating will drive the temperature of the gas above the virial temperature. If the gas is unable to cool efficiently, this increase in temperature will lead to a decrease in accretion rate by either decreasing the radius of the sonic point or by driving a thermal outflow.

Motivated by these considerations, this paper as-

sesses the importance of thermal conduction using a simple one-dimensional (spherical) model of hot accretion flows with saturated conduction. Tanaka & Menou (2006) have carried out a related analysis and find that the accretion flow can spontaneously produce thermal outflows driven in part by conduction (as in early models of the solar wind). Their analysis is two-dimensional but self-similar in radius, whereas ours is one-dimensional but does not assume self-similarity; we also treat saturated heat conduction somewhat differently than they do (see §2). Tanaka & Menou’s assumption of self-similarity enforces a density profile that varies as $r^{-3/2}$, whereas simulations of RIAFs consistently find density profiles shallower than this (e.g., Stone et al. 1999, Igumenshchev & Abramowicz 1999, Stone & Pringle 2001, Hawley & Balbus 2002, Igumenshchev et al. 2003).

We begin in §2 by outlining the energy equation in the presence of saturated heat conduction. For completeness we consider both the ion and electron energy equations, though our focus will be on the electrons throughout this paper; we also quantify when electron heat conduction is likely to be important as an energy transport mechanism relative to radiative cooling. We then present order of magnitude arguments that demonstrate the importance of heat conduction in hot accretion flows. In particular, we solve for the electron temperature in the presence of heat conduction under the simplifying assumption that the density profile of the accretion flow is a fixed power-law in radius (§3). In §4 we relax the power-law density profile assumption of §3 and self-consistently solve for the density, temperature, and radial velocity of the flow neglecting angular momentum; this is a version of the classic Bondi (1952) accretion problem. We summarize and discuss the implications of our findings in §5.

2. ENERGY EQUATIONS

As noted in the Introduction, in a hot accretion flow the timescale for electrons and ions to exchange energy by Coulomb collisions exceeds the timescale for the plasma to flow into the central black hole. Thus the flow likely develops a two-temperature structure, although the extent to which the particle species are coupled through other processes such as wave-particle interactions is unclear. In general, then, the energy of the electrons and ions must be tracked separately. In spherical symmetry, the electron and ion energy equations can be written as

$$-v_r n T_e \frac{ds_e}{dr} = q_e^+ - \frac{1}{r^2} \frac{d}{dr} (r^2 Q_e) - q_e^-, \quad (1)$$

and

$$-v_r n T_i \frac{ds_i}{dr} = q_i^+ - \frac{1}{r^2} \frac{d}{dr} (r^2 Q_i) \quad (2)$$

where $v_r \equiv -dr/dt$ is the radial velocity (defined here to be positive inward), n is the particle number density ($n_e = n_i \equiv n$ by charge neutrality, where the subscripts e and i denote properties of the electron and ion fluids, respectively), s is the specific entropy, q^+ is the heating rate per unit volume, and q_e^- is the electron cooling rate per unit volume.¹ In equations (1) and (2) we have ne-

glected energy exchange between ions and electrons (e.g., via Coulomb collisions) and ion radiative cooling. The last term on the right-hand side of equations (1) and (2) is the divergence of the radial conductive heat flux

$$Q_{e,i} \equiv -\kappa_{e,i} \frac{dT_{e,i}}{dr}. \quad (3)$$

Because the accreting plasma is collisionless, we model the thermal conductivity κ using a saturated thermal conductivity (Cowie & McKee 1977):

$$\kappa_e \equiv \alpha_c v_c n r, \quad (4)$$

where α_c is a dimensionless parameter that measures the strength of the conduction and

$$v_c \equiv \frac{c v_e}{c + v_e} \simeq \begin{cases} v_e & \text{for } v_e \ll c \\ c & \text{for } v_e \gg c \end{cases} \quad (5)$$

is a function that interpolates smoothly between the electron thermal speed at low temperatures and the speed of light c as the electrons become relativistic. For the ions, which are always non-relativistic, $\kappa_i \equiv \alpha_c v_i n r$ where v_i is the ion thermal velocity. We use a slightly different form for the saturated flux than Cowie & McKee (1977). Their flux is proportional to density and temperature, while we take the flux to be proportional to the temperature gradient. For our problem, the temperature and density are boundary conditions at large radii; the Cowie & McKee (1977) prescription would lead to the heat flux being specified by these boundary conditions, which is unphysical since we want to be able to solve for the heat flux rather than have it predetermined. We note, however, that our assumption of $Q \propto dT_e/dr$, while physically reasonable, cannot be rigorously derived in the collisionless limit, where the heat flux depends on a non-local integral of the electron temperature along magnetic field lines (see, e.g., §VII of Snyder et al. 1997).²

Assuming that a fraction f_e (f_i) of the available accretion energy goes into heating the electrons (ions), the electron and ion heating rates per unit volume are given by

$$q_{e,i}^+ = f_{e,i} \frac{GM\dot{M}}{4\pi r^4}. \quad (6)$$

where $f_i = 1 - f_e$. Integrating the total (electron + ion) volumetric heating rate over all radii yields a net heating rate of $GM\dot{M}/R_{in}$, where R_{in} is the inner radius of the flow. We set $R_{in} = 3R_S = 6GM/c^2$ throughout this paper so that the total heating rate is $\approx 0.16M\dot{c}^2$. Note that even for spherical accretion (i.e., in the absence of differential rotation and the MRI), a significant fraction of the gravitational potential energy of the inflowing gas may be converted into heat. In particular, even initially weak magnetic fields are compressed by flux freezing until they become strong, leading to reconnection and significant heating (Igumenshchev & Narayan 2002).

Because $v_e \gg v_i$ unless $T_e \lesssim 10^{-3} T_i$, electron heat conduction tends to be more important than ion heat conduction. Our focus in this paper will thus be on electron heat conduction. We note, however, that electron

results in Kelvin.

² If wave-particle scattering limits the mean free path of particles to be $\lesssim r$ at any radius, then $Q \propto dT_e/dr$ is again well-justified.

¹ We work in units in which Boltzmann’s constant $k_B \equiv 1$ so that temperature has units of energy, although we express our numerical

heat conduction is important only when electron radiative losses are relatively small. Otherwise, most of the energy supplied to the electrons is radiated away and there is little energy available to redistribute by conduction. Throughout this paper we thus set $q_e^- = 0$ in equation (1). This is valid only when the cooling time of the electrons in the accretion flow is long compared to the conduction time, r/v_c . At the low accretion rates where this assumption is appropriate (see below), and inside $\sim 10^3 R_S$ where the electrons are relativistic, synchrotron cooling is the dominant cooling mechanism (e.g., Quataert & Narayan 1999). Synchrotron cooling for thermal electrons at temperature T_e can be neglected only for

$$\frac{\dot{M}}{\dot{M}_{\text{EDD}}} \lesssim 10^{-6} \left(\frac{\beta}{10}\right) \left(\frac{\alpha_c}{0.1}\right) \left(\frac{\alpha}{0.1}\right) \left(\frac{T_e}{10^{11} \text{ K}}\right)^{-1} \left(\frac{r}{3R_S}\right)^{3/2}, \quad (7)$$

where $\dot{M}_{\text{EDD}} \equiv L_{\text{EDD}}/(0.1c^2)$ is the Eddington accretion rate, the radial velocity is assumed to be a fraction α of the free-fall velocity, the magnetic field has been normalized to the virial temperature via $\beta \equiv nT_i/(B^2/8\pi)$, the average Lorentz factor for a thermal distribution of electrons is given by $3T_e/(m_e c^2)$, and $v_c \approx c$ for relativistic electrons. Expression (7) is considerably more restrictive than the requirement that $\dot{M} \lesssim \alpha^2 \dot{M}_{\text{EDD}}$ for Coulomb collisions to be unimportant, which is necessary to maintain a two-temperature flow (Rees et al. 1982). There is therefore a large range of accretion rates where a RIAF is possible but where electron heat conduction is unimportant because the electrons radiate away most of their energy.³ Our focus here is on very low accretion-rate systems where electron radiative losses are small. This includes Sgr A* in the Galactic Center and other very low-luminosity AGN and X-ray binaries in quiescence. Ion heat conduction may be important at higher accretion rates, but this is harder to assess because the ion conduction time is comparable to the inflow time.

We note that in their treatment of heat conduction in RIAFs, Tanaka & Menou (2006) use a single energy equation, as we do. Interpreted as electron conduction, their results—like ours—are only relevant for very low accretion rates. Interpreted as ion conduction, their ϕ_S should be $\lesssim 0.01$ (and their $\lambda_0 \lesssim 0.1$) since using the ion thermal speed in the conductivity introduces an additional factor of $\sqrt{m_e/m_p}$. For these values, their solutions show that ion conduction has only a modest effect on the properties of RIAFs.

The appropriate values for α_c and f_e are set by complicated physical processes that are not fully understood. The electron heating parameter must satisfy $f_e \lesssim 1$ on energetic grounds. For reasons explained in, e.g., Quataert & Gruzinov (1999) and Quataert (2003), we suspect that the electrons likely receive a significant fraction of the available gravitational potential energy in RIAFs, so that $f_e \sim 0.1 - 1$ is reasonable. The dimensionless conductivity α_c must also satisfy $\alpha_c \lesssim 1$. We show solutions with $\alpha_c \gtrsim 1$, however, in order to illustrate the change in dynamics as the inflowing plasma

³ Note that at high accretion rates electron conduction could still be important at radii $\gtrsim 10^3 R_S$ where the electrons are non-relativistic and synchrotron losses are small.

becomes isothermal. In the Appendix we place an upper limit on the ion conductivity of $\alpha_c \lesssim 0.1$ based on pitch angle scattering by instabilities generated by the nonlinear evolution of the MRI in a collisionless plasma. This argues against the importance of ion conduction. The corresponding constraint on the electron conductivity is much weaker (eq. A3).

With equations (1)-(6) describing the electron energetics, we now proceed to assess the importance of heat conduction in RIAFs by considering a couple of model problems.

3. ORDER-OF-MAGNITUDE CONSIDERATIONS

To quantitatively motivate the importance of thermal conduction, we consider a simple model in which a fraction f_e of the accretion energy ($0.1\dot{M}c^2$) is carried out to large radii by a saturated conductive heat flux with $\alpha_c \sim 1$, in which case $0.1f_e\dot{M}c^2 \approx 4\pi pr^2 v_e^3 (m_e/m_p)$. For constant \dot{M} , this implies

$$\frac{T_e}{T_{\text{vir}}} \sim \left(0.1f_e \sqrt{\frac{m_e}{m_p}} \frac{r}{R_S}\right)^{2/3} \sim 30 \left(f_e \frac{r}{10^5 R_S}\right)^{2/3}, \quad (8)$$

where we have assumed that the electrons are non-relativistic, which is true at large radii, $r/R_S \gtrsim 10^3$. Equation (8) shows that if even a small fraction of the available energy is transported outwards by conduction ($f_e \gtrsim 0.01$), the heat flux can unbind the gas at large radii, thus significantly changing the flow dynamics.

The above analysis assumes that \dot{M} is constant and thus that the density profile of the flow is given by $\rho \propto r^{-3/2}$, the canonical result for spherical accretion. Models of rotating radiatively inefficient accretion flows show, however, that the dynamics of the flow can be quite different from that of spherical accretion. In particular, convection (Stone et al. 1999; Quataert & Gruzinov 2000a; Narayan et al. 2000) and/or thermally driven winds (Blandford & Begelman 1999; Stone & Pringle 2001; Hawley & Balbus 2002) can strongly suppress the rate of mass accretion onto the central black hole. A simple model for such a flow is one in which the density profile is given by $n \propto r^{-p}$, so that $\dot{M} \propto r^{3/2-p}$ is steady in time but varies with radius. Numerical simulations favor $p \approx 1/2 - 1$. For $p < 3/2$, the mass accretion rate decreases at small radii, and there is *less* energy available to be conducted out to large radii. In this case, energy transport by conduction has less of an effect on the dynamics of the flow. To quantify this, we again assume that a fraction f_e of the accretion energy at small radii ($0.1\dot{M}[R_S]c^2$) is carried out to large radii by a saturated conductive heat flux; allowing for $\dot{M} \propto r^{3/2-p}$, the temperature at large radii is given by

$$\frac{T_e}{T_{\text{vir}}} \sim \left(\frac{0.1f_e}{p-1/2} \sqrt{\frac{m_e}{m_p}} \left[\frac{r}{R_S}\right]^{p-1/2}\right)^{2/3} \quad (9)$$

for $p > 1/2$ and

$$\frac{T_e}{T_{\text{vir}}} \sim \left(0.1f_e \sqrt{\frac{m_e}{m_p}} \ln \left[\frac{r}{R_S}\right]\right)^{2/3} \quad (10)$$

for $p = 1/2$. For $p = 1/2$, equation (10) shows that the

electron temperature required to carry the heat flux out is always sub-virial and thus conduction is not dynamically important. More generally, from equation (9), and assuming a fiducial outer-radius of $r \sim 10^5 R_S$, we find that the electron temperature is super-virial for $p \gtrsim 1$.

To expand on the above analysis, we solve the full electron energy equation (eq. [1]) using a standard relaxation algorithm (Press et al. 1992) for a fixed density profile $n \propto r^{-p}$. We take the radial velocity to be given by

$$v_r \equiv \alpha \left(\frac{H}{r} \right)^2 v_\phi \simeq \alpha \sqrt{\frac{GM}{r}}, \quad (11)$$

where $H \simeq r$ is the vertical scale-height for a hot accretion flow, $v_\phi = r\Omega$ is the rotational velocity and $\Omega = \sqrt{GM/r^3}$ is the Keplerian rotational frequency. There are two boundary conditions for this problem since we are specifying both the radial velocity and density profiles. A reasonable set of boundary conditions is to specify the temperature at the outer radius and to require that $dT_e/dr|_{R_{in}} = 0$, i.e., that the conductive heat flux is zero at the inner radius (so that there is not a source of energy at the horizon). Our results are all insensitive to the precise inner boundary condition (for modest values of $dT_e/dr|_{R_{in}}$). The parameters that determine the electron temperature in this model are α_c/α , p , and f_e .

Figure 1 is a plot of $T_e(r)$ for different choices for the density power-law index p . The values for the other parameters are $\alpha_c/\alpha = 1$, $f_e = 0.1$ and an outer temperature $T_{out} = 2 \times 10^7$ K (the temperature observed in the Galactic Center; Baganoff et al. 2003). Figure 1 shows that larger values of p lead to larger electron temperatures (see also eqs. [8]-[10]). This is because larger values of p correspond to larger accretion rates and electron heating rates at small radii. In the presence of significant heat conduction some of the energy supplied to the electrons at small radii is conducted to large radii (for $\alpha_c \sim \alpha$, the heat conduction time is $\sim v_c/v_\phi \gtrsim 1$ times smaller than the inflow time; thus most of the energy supplied to the electrons is conducted to large radii, as assumed in the order of magnitude estimates above). Larger values of p thus correspond to a larger heat flux at large radii, and a larger electron temperature is needed to carry this heat flux (eqs. [3]-[5] imply $Q_r \propto T_e^{3/2}$ at large radii where the electrons are non-relativistic). For sufficiently large values of $p \gtrsim 1$ the solutions shown in Figure 1 are unphysical: the electron temperature becomes super-virial, indicating that the electron pressure gradient is dynamically important and that the electrons are unbound from the system (see also eq. [9]).

Using solutions with $p = 1$ and $p = 1/2$ as reference calculations (values motivated in part by simulations of RIAFs), we explore how the temperature profile varies as a function of α_c/α and f_e . These calculations are shown in Figures 2 and 3. The trends in these figures can all be understood relatively easily. Larger values of f_e correspond to larger electron heating rates and thus lead to higher electron temperatures. Larger values of α_c/α , on the other hand, correspond to very efficient heat conduction that drives the electron temperature profile towards isothermality. Note that in the case of $p = 1/2$, the electron temperature is never super-virial (Fig. 3), consistent with our order-of-magnitude estimate in equation (10).

4. SPHERICAL ACCRETION WITH CONDUCTION

The fact that the electron temperature calculated in the previous section is sometimes super-virial implies that conduction can significantly influence the dynamics of the accretion flow; this motivates the investigation of this subsection, in which we solve for the density and velocity profiles self-consistently. We consider a simple model of a hot accretion flow, assuming spherical symmetry, constant \dot{M} , and neglecting angular momentum.

With the above assumptions the basic dynamical equations for the density and radial velocity are

$$\dot{M} = 4\pi r^2 \rho v_r, \quad (12)$$

$$v_r \frac{dv_r}{dr} + \frac{1}{\rho} \frac{dP_e}{dr} + \frac{GM}{(r - R_S)^2} = 0, \quad (13)$$

where P_e is the electron pressure and we have used the Paczynsky & Wiita (1980) gravitational potential to ensure that all the solutions have a sonic radius outside the horizon. In addition to equations (12) and (13) we solve equation (1) for the electron temperature, which can also be written as

$$nv_r \frac{d}{dr} \left(\frac{T_e}{\gamma_e - 1} \right) - v_r T_e \frac{dn}{dr} + \frac{f_e GM m_p n v_r}{r^2} + \frac{\alpha_c}{r^2} \frac{d}{dr} \left(r^3 n v_c \frac{dT_e}{dr} \right) = 0, \quad (14)$$

where the entropy gradient has been rewritten in terms of density and temperature gradients and the internal energy has been expressed in terms of an effective adiabatic index

$$\gamma_e \equiv \left(\frac{10}{3} \right) \left(\frac{1 + 2v_e^2/c^2}{2 + 5v_e^2/c^2} \right) \simeq \begin{cases} 5/3 & \text{for } v_e \ll c \\ 4/3 & \text{for } v_e \gg c \end{cases} \quad (15)$$

that interpolates smoothly between nonrelativistic and relativistic energies. Equations (12)-(14) are the Bondi (1952) accretion problem except that there is now explicit heating and an additional dependent variable (dT_e/dr) due to the conductive flux term in equation (14). We note that Gruzinov (1998) has also considered Bondi accretion in the presence of heat conduction, although his form of the conductive heat flux is quite different from ours and leads to different results.

In general, the pressure in equation (13) is given by the sum of the electron and ion gas pressures (radiation pressure is negligible since the plasma is optically thin and we do not include the effects of magnetic fields) and one needs to solve equation (2) for the ions in addition to equation (14) for the electrons. Since our goal is to understand the effects of conduction on the solution, however, it is reasonable to neglect the ion pressure in equation (13) and focus solely on the electron energetics. The ion temperature in hot accretion flows is approximately virial, $T_i \propto 1/r$, where the constant of proportionality depends upon the assumption one makes about the fraction f_i of accretion energy that goes into heating the ions. In §5, we briefly discuss the effect of including the ion energy equation in our solutions.

Eliminating the density as a dependent variable in favor of the radial velocity, the momentum equation can be expressed as

$$(v_r^2 - c_s^2) \frac{1}{v_r} \frac{dv_r}{dr} = \frac{2c_s^2}{r} - \frac{dc_s^2}{dr} - \frac{GM}{(r - R_S)^2}, \quad (16)$$

where $c_s^2 \equiv P_e/\rho$ is the isothermal sound speed. Equation (16) is singular when the factor in parentheses on the left-hand side is zero. By analogy with the Bondi problem, we expect a family of subsonic solutions as well as a unique solution that makes a transition between subsonic and supersonic flow at an intermediate radius R_{sonic} (the sonic point). The solution that passes through the sonic point is selected by setting both the left-hand and right-hand sides of equation (16) to zero at R_{sonic} . Specifying two additional boundary conditions over-constrains the problem, so that R_{sonic} (and therefore \dot{M}) is uniquely determined as an eigenvalue. As in the previous section, the additional two boundary conditions are the temperature at the outer radius T_{out} and the zero-flux condition ($dT_e/dr = 0$) at the inner radius. Note that the problem solved in this section is thus a 3 point boundary value problem, with boundary conditions at the inner radius, sonic point, and outer radius. We solve this problem with a relaxation algorithm.

Figures 4, 5 and 6 show the temperature, density and velocity profiles for a set of calculations with $f_e = 0.3$, $T_{out} = 2 \times 10^7$ K and various values of α_c . Our choice of T_{out} corresponds to a gravitational sphere of influence of the black hole of $GM/c_s^2|_{R_{out}} \approx 10^5 R_S$. As in Figures 2 and 3, large values of α_c drive the electron temperature to be isothermal. The electron temperature is maximized (and the density at small radii minimized) for $\alpha_c \sim 1$. The differences relative to the standard Bondi problem are quantified more clearly in Figures 7 and 8, which show the sonic radius and accretion rate as a function of α_c for several values of f_e . In all of our calculations, the standard Bondi problem is recovered as $\alpha_c \rightarrow 0$ and $f_e \rightarrow 0$, though note that we are employing an adiabatic index that varies with radius so the $\alpha_c \rightarrow 0$ solution does not correspond to a constant γ as in the Bondi problem. In the limit of infinite conductivity, $\alpha_c \gg 1$, the electron temperature profile becomes isothermal, independent of f_e , and the problem reduces to the standard Bondi problem with $\gamma = 1$.

For intermediate values of $\alpha_c \sim 1$, however, the solution differs significantly from the canonical Bondi solution. In particular, Figure 7 shows that for moderate values of f_e and $\alpha_c \sim 0.1 - 1$, the sonic point moves in from $\sim 10^5 R_S$ to $\sim 10 - 100 R_S$. The accretion rate is correspondingly reduced relative to the adiabatic or isothermal Bondi rate by $\sim 1 - 3$ orders of magnitude (Fig. 8). Physically, this occurs because accretion at the Bondi rate would imply so much heat conduction to large radii that the electron temperature would be super-virial, as found in the previous section. To maintain $T_e \lesssim T_{vir}$ requires that the accretion rate decrease so that less energy is conducted out to large radii. This occurs via a decrease in the radial velocity (Fig. 6) relative to free fall and a flattening of the radial density profile relative to the $r^{-3/2}$ Bondi solution (Fig. 5).

The fact that the accretion rate for nonzero f_e differs from the adiabatic Bondi rate at low α_c can be understood as follows. In the outer, subsonic region, the momentum equation is dominated by hydrostatic balance:

$$\frac{d(nT_e)}{dr} + \frac{GMm_p n}{r^2} = 0. \quad (17)$$

For $\alpha_c = 0$, the energy equation is given by

$$n \frac{d}{dr} \left(\frac{T_e}{\gamma_e - 1} \right) - T_e \frac{dn}{dr} + \frac{f_e GMm_p n}{r^2} = 0. \quad (18)$$

Combining these two relations gives

$$\frac{d}{dr} \left[\frac{\gamma_e}{\gamma_e - 1} T_e - \frac{GMm_p}{r} - f_e \frac{GMm_p}{r} \right] = 0, \quad (19)$$

which for the form of γ_e we have chosen gives a quadratic relation for T_e . For constant γ , $T_e \propto 1/r$ and $n \propto r^{-p}$, with

$$p = \frac{1 - f_e(\gamma - 1)}{(1 + f_e)(\gamma - 1)}. \quad (20)$$

The assumption of hydrostatic equilibrium breaks down for $p > 3/2$ (the free-fall value), or

$$\gamma < \gamma_{crit} \equiv \frac{5(1 + f_e)}{3(1 + 5f_e/3)}. \quad (21)$$

For $\gamma < \gamma_{crit}$ a supersonic free-fall solution is obtainable, while for larger γ it is not. Since $\gamma_{crit} < 5/3$ for nonzero f_e , the assumption of hydrostatic equilibrium holds for a larger range of radii than it would in the absence of heating (until the temperature increases and γ_e decreases enough to violate condition [21]). There is a corresponding decrease in the sonic radius and accretion rate even for $\alpha_c \rightarrow 0$, as can be seen in Figures 7 and 8. Also, since $\gamma_e > 4/3$, equation (21) indicates that only solutions with $f_e < 0.6$ will be able to make a transition to supersonic flow as $\alpha_c \rightarrow 0$ (in a Newtonian potential). For larger values of f_e the flow is in approximate hydrostatic equilibrium down to very small radii, where the singularity in the pseudo-Newtonian potential forces a sonic transition.

5. DISCUSSION

We have shown that electron heat conduction can have a significant effect on the properties of radiatively inefficient accretion flows (RIAFs). We considered two model problems to demonstrate this, both of which assume spherical symmetry. First, for the canonical Bondi problem, we find that if a few percent of the accretion power is transferred to large radii by heat conduction, the heat flux can unbind the gas at large radii (eq. [8]). Generalizing this calculation to allow for a power-law density profile with $n(r) \propto r^{-p}$ (§3 and Figs. 1-3), we solved for the electron temperature profile in the presence of saturated heat conduction; $p = 3/2$ is appropriate for the spherical Bondi problem, while $p \sim 1/2 - 1$ is typically found in numerical simulations of rotating radiatively inefficient accretion flows. Our calculations show that for density profiles with $p \gtrsim 1$, and for plausible values of the electron conductivity and electron heating, the electron temperature is super-virial at large radii (see Fig. 1-3). This indicates that the effects of conduction on the dynamics of the accretion flow must be self-consistently taken into account.

Motivated by this initial calculation, we solved the problem of spherical accretion in the presence of heat conduction and electron heating. For appreciable electron heating rates ($f_e \sim 0.1$) and dimensionless conductivities $\alpha_c \sim 0.1 - 1$ (see §2 for the details of the electron energy equation), the accretion rate is reduced by $\sim 1 - 3$

orders of magnitude relative to the canonical Bondi rate (§4; Fig. 8). Physically, this is because some of the energy dissipated as heat is conducted to large radii where the increase in pressure stifles the inflow of matter. This decrease in \dot{M} relative to the Bondi accretion rate is consistent with observations of the Galactic Center, which indicate that the accretion rate is 2 – 3 orders of magnitude lower than the Bondi rate (Quataert & Gruzinov 2000b; Bower et al. 2003; Marrone et al. 2006).

As discussed in §2, electron heat conduction is only important at very low accretion rates $\lesssim 10^{-5} - 10^{-6} M_{\text{EDD}}$, when the cooling time of the electrons via synchrotron radiation is longer than the conduction time in the plasma (eq. [7]). Such accretion rates are appropriate for very low-luminosity AGN such as Sgr A* in the Galactic Center, massive black holes in early type galaxies (e.g., Di Matteo et al. 2000), and some X-ray binaries in quiescence. For higher accretion rates, the electrons cool more rapidly than energy can be redistributed by conduction, and so electron conduction is unimportant. Ion heat conduction could in principle be relevant at all accretion rates since the ion cooling time in RIAFs is always longer than the inflow time (by construction); this is, however, harder to quantify because the ion conduction time is at best comparable to the inflow time of the plasma.

All of the calculations in this paper assume spherical symmetry. This is formally appropriate only in the absence of significant angular momentum, when the circularization radius of the inflowing material is small compared to the gravitational sphere of influence of the central object. We suspect, however, that the calculations presented here are relevant to rotating accretion flows as well, given the importance of energy transport in determining the structure of RIAFs (e.g., Blandford & Begelman 1999). In a rotating accretion disk, however, the conducted energy may be transported to the surface of the disk, rather than to large radii. This conductive flux might contribute to driving a thermal outflow. Indeed, the two-dimensional calculations of Tanaka & Menou (2006) indicate that conduction helps drive a bipolar outflow. Numerical simulations of RIAFs with heat conduction are necessary to further quantify the importance of conduction and to assess whether any resulting heat flux is primarily radial or vertical. Existing simulations of RIAFs – which do not include thermal conduction – find density profiles with $p \approx 1/2 - 1$, in which case our calculations indicate that conduction is unlikely to lead to super-virial temperatures which would be dynamically important (see Figs. 1-3). Even in this case, however, conduction would be important for determining the electron temperature profile and thus the observed radiation.

Throughout this paper we have treated the dimensionless conductivity α_c as a free parameter in order to explore the effects of conduction in RIAFs. A precise determination of α_c in this context requires understanding the effective conductivity in a magnetized, turbulent plasma. Wave-particle scattering by high frequency turbulence can limit the mean free path of particles in low collisionality plasmas, and thus the conductivity. In the Appendix, we argue that instabilities generated by the nonlinear evolution of the MRI in RIAFs lead to an up-

per limit on the ion conductivity of $\alpha_c \lesssim 0.1$, in which case ion conductivity is unlikely to be dynamically important. We find that there is no corresponding limit on the electron conductivity, although a large heat flux itself may be self-limiting by generating whistler instabilities (e.g., Pistinner & Eichler 1998). Independent of wave-particle scattering, electron transport perpendicular to a static magnetic field is suppressed due to the small value of the electron Larmor radius. However, the rapid separation of neighboring field lines in a turbulent medium results in an effective isotropic conductivity comparable to the field-free conductivity (Jokipii 1973; Narayan & Medvedev 2001; Cho & Lazarian 2004; Chandran & Maron 2004; Maron et al. 2004). This suggests that electron heat conduction will be dynamically important even in the presence of a tangled magnetic field, with $\alpha_c \sim 0.1 - 1$. With this value of the electron conductivity, we find that conduction significantly modifies the dynamics of Bondi accretion (see Figs. 7-8).

Balbus (2000) has shown that low collisionality conducting plasmas are unstable to convective-like motions in the presence of an outwardly decreasing temperature gradient (the MTI). In a non-rotating atmosphere, Parrish & Stone (2005) demonstrate that the MTI leads to magnetic field amplification and a substantial heat flux down the temperature gradient. It is natural to speculate that our solutions represent the non-linear saturation of the MTI in accretion disks. However, simulations of the MTI in RIAFs are necessary to test this hypothesis since it is not clear what effect differential rotation and the MRI will have on the results of Parrish & Stone (2005). The MTI will also be important in purely spherical accretion, as indicated by Figure 9, which shows the growth rate of the MTI in units of the inverse infall time calculated from one of our spherical accretion solutions with $f_e = 0$ and $\alpha_c = 0.1$. As Figure 9 shows, the MTI will be particularly important at large radii and will likely significantly modify existing results on the impact of magnetic fields on spherical accretion (e.g., those of Igumenshchev & Narayan 2002).

Although our focus in this paper is on the electron energetics in RIAFs, we have also carried out some preliminary calculations including the ions (neglecting ion conduction for reasons discussed above and in §2). For spherical accretion with significant ion heating, the accretion rate is reduced relative to the Bondi rate by even more than is shown in our electron-only calculations in Figure 8. This is consistent with the arguments in §4. The ions are non-relativistic throughout most of the flow, and therefore have $\gamma_i \simeq 5/3$. In the presence of ion heating, the effective adiabatic index of the flow is $\gtrsim 5/3$, in which case there is no transonic Bondi solution in Newtonian gravity. Instead, the inflowing matter is in approximate hydrostatic equilibrium throughout the bulk of the flow and the solution never achieves the free-fall density profile of $\rho \propto r^{-3/2}$ (see the discussion around eq. [21]). The further reduction in accretion rate due to the inclusion of ion heating (even absent ion conduction), while strengthening our conclusions, is a consequence of the singular nature of the $\gamma_i \simeq 5/3$ Bondi solution, for which $R_S \simeq 0$. Including additional physical effects such as rotation will partially remove this singular behavior and may be required to realistically assess the impact of ion heating and conduction on the dynamics of hot

accretion flows.

As noted in the Introduction, radiation emitted from close to the accreting object can play a role analogous to that of conduction in heating up the outer region of the accretion flow to super-virial temperatures. This mechanism has been studied in the context of RI-AFs by Park & Ostriker (1998, 1999, 2001). The accretion flow in that case can exhibit time dependence due to the lack of a steady-state solution or to thermal instability (Ostriker et al. 1976; Cowie et al. 1978; Bisnovatyi-Kogan & Blinnikov 1980; Krolik & London 1983). We do not expect time dependence in our problem, since our calculations show that a steady-state solution does exist and conduction tends to stabilize thermal instabilities (Krolik & London 1983); a time-dependent

calculation or a stability analysis would, however, be required to confirm this. We also note that our calculations are only relevant for systems with sufficiently low luminosities as to be unaffected by radiative preheating (as discussed above, our solutions require low luminosities so that a significant fraction of the accretion energy can be conducted outwards rather than being radiated away).

We thank Steve Balbus, Greg Hammett, Kristen Menou, Prateek Sharma, and the referee, Jerry Ostriker, for useful conversations and comments. This work was supported in part by NSF grant AST 0206006, NASA grant NAG5-12043, an Alfred P. Sloan Fellowship, and the David and Lucile Packard Foundation.

REFERENCES

- Balbus, S. A. 2000, *ApJ*, 534, 420
 Bisnovatyi-Kogan, G. S., & Blinnikov, S. I. 1980, *MNRAS*, 191, 711
 Blandford, R. D., & Begelman, M. C. 1999, *MNRAS*, 303, L1
 Bondi, H. 1952, *MNRAS*, 112, 195
 Bower, G. C., Wright, M. C. H., Falcke, H., & Backer, D. C. 2003, *ApJ*, 588, 331
 Chandran, B. D. G., & Maron, J. L. 2004, *ApJ*, 602, 170
 Chapeau-Blondeau, F. & Monir, A. 2002, *IEEE Transactions on Signal Processing*, 50(9), 2160
 Cho, J., & Lazarian, A. 2004, *Journal of Korean Astronomical Society*, 37, 557
 Cowie, L. L., & McKee, C. F. 1977, *ApJ*, 211, 135
 Cowie, L. L., Ostriker, J. P., & Stark, A. A. 1978, *ApJ*, 226, 1041
 Di Matteo, T., Quataert, E., Allen, S. W., Narayan, R., & Fabian, A. C. 2000, *MNRAS*, 311, 507
 Gary, S. P., Lee, M. A. 1994, *J. Geophys. Res.*, 99, 11297
 Gary, S. P., Wang, J., 1996, *JGR*, 101, 10749
 Gary, S. P., Wang, J., Winske, D., & Fuselier, S. A. 1997, *J. Geophys. Res.*, 102, 27159
 Gruzinov, A. V. 1998, *astro-ph/9809265*
 Hawley, J. F., & Balbus, S. A. 2002, *ApJ*, 573, 738
 Igumenshchev, I. V., & Abramowicz, M. A. 1999, *MNRAS*, 303, 309
 Igumenshchev, I. V., & Narayan, R. 2002, *ApJ*, 566, 137
 Igumenshchev, I. V., Narayan, R., & Abramowicz, M. A. 2003, *ApJ*, 592, 1042
 Jokipii, J. R. 1973, *ApJ*, 183, 1029
 Krolik, J. H., & London, R. A. 1983, *ApJ*, 267, 18
 Lynden-Bell, D. 1969, *Nature*, 223, 690
 Marrone, D. P., Moran, J. M., Zhao, J.-H., & Rao, R. 2006, *ApJ*, 640, 308
 Maron, J., Chandran, B. D., & Blackman, E. 2004, *Physical Review Letters*, 92, 045001
 Narayan, R., Igumenshchev, I. V., & Abramowicz, M. A. 2000, *ApJ*, 539, 798
 Narayan, R., & Medvedev, M. V. 2001, *ApJ*, 562, L129
 Narayan, R., & Yi, I. 1994, *ApJ*, 428, L13
 Ostriker, J. P., Weaver, R., Yahil, A., & McCray, R. 1976, *ApJ*, 208, L61
 Paczynsky, B., & Wiita, P. J. 1980, *A&A*, 88, 23
 Park, M.-G., & Ostriker, J. P. 1998, *Advances in Space Research*, 22, 951
 Park, M.-G., & Ostriker, J. P. 1999, *ApJ*, 527, 247
 Park, M.-G., & Ostriker, J. P. 2001, *ApJ*, 549, 100
 Parrish, I. J., & Stone, J. M. 2005, *ApJ*, 633, 334
 Pistinner, S. L., & Eichler, D. 1998, *MNRAS*, 301, 49
 Press, W. H., Teukolsky, S. A., Vetterling, W. T., & Flannery, B. P. 1992, Cambridge: University Press, —c1992, 2nd ed.
 Quataert, E. 2003, *Astronomische Nachrichten Supplement*, 324, 435
 Quataert, E. 2004, *ApJ*, 613, 322
 Quataert, E., & Gruzinov, A. 1999, *ApJ*, 520, 248
 Quataert, E., & Gruzinov, A. 2000a, *ApJ*, 539, 809
 Quataert, E., & Gruzinov, A. 2000b, *ApJ*, 545, 842
 Quataert, E., & Narayan, R. 1999, *ApJ*, 520, 298
 Rees, M. J., Phinney, E. S., Begelman, M. C., & Blandford, R. D. 1982, *Nature*, 295, 17
 Salem, C., Hubert, D., Lacombe, C., Bale, S. D., Mangeney, A., Larson, D. E., & Lin, R. P. 2003, *ApJ*, 585, 1147
 Shakura, N. I., & Sunyaev, R. A. 1973, *A&A*, 24, 337
 Sharma, P., Hammett, G. W., Quataert, E., & Stone, J. M. 2006, *ApJ*, 637, 952
 Snyder, P. B., Hammett, G. W., & Dorland, W. 1997, *Physics of Plasmas*, 4, 3974
 Stix, T. H. 1992, *Waves in Plasmas*, AIP Press
 Stone, J. M., Pringle, J. E., & Begelman, M. C. 1999, *MNRAS*, 310, 1002
 Stone, J. M., & Pringle, J. E. 2001, *MNRAS*, 322, 461
 Tanaka, T., & Menou, K. 2006, *ApJ* accepted, *astro-ph/0604509*

APPENDIX
AN UPPER LIMIT ON α_c

In a collisionless plasma, the temperature and pressure need not be the same perpendicular (T_\perp) and parallel (T_\parallel) to the local magnetic field. The temperature anisotropy cannot, however, be arbitrarily large because high frequency waves and kinetic microinstabilities feed on the free energy in the temperature anisotropy, effectively providing an enhanced rate of collisions that isotropizes the pressure tensor via pitch angle scattering. This in turn limits the mean free-path of particles and thus the heat conductivity. These issues are discussed in detail in Sharma et al. (2006) in the context of nonlinear simulations of the MRI in a collisionless plasma. Here we use this effect to estimate an upper limit on α_c for ions and electrons in RIAFs. For concreteness we focus on instabilities generated by $T_\perp > T_\parallel$. For conditions appropriate to RIAFs, the most important instability regulating the ion (electron) pressure anisotropy is the ion cyclotron (whistler) instability.⁴

For electromagnetic fluctuations slow compared to the cyclotron frequency, the magnetic moment ($\mu \propto T_\perp/B$) is an adiabatic invariant. As a result, temperature anisotropies with $T_\perp \neq T_\parallel$ are created due to the fluctuating magnetic field associated with the MRI. Formally, a plasma with any nonzero temperature anisotropy can be unstable to the ion cyclotron and whistler instabilities (Stix 1992). However, there is an effective anisotropy threshold given by the requirement that the unstable modes grow on a timescale comparable to the disk rotation period. Gary and collaborators have analyzed the ion cyclotron instability in detail through linear analysis and numerical simulations. Gary et al. (1997) and Gary & Lee (1994) calculate the anisotropy required for a given growth rate γ relative to the ion cyclotron frequency Ω_i

$$\frac{p_\perp}{p_\parallel} - 1 > \frac{S}{\beta_{\parallel,i}^q} \quad (\text{A1})$$

where $\beta_{\parallel,i} = p_{\parallel,i}/(B^2/8\pi)$ and where $S = 0.35$ and $q = 0.42$ are fitting parameters quoted in equation (2) of Gary & Lee (1994) for $\gamma/\Omega_i = 10^{-4}$. Moreover, for $\gamma \ll \Omega_i$ the threshold anisotropy depends only very weakly on the growth rate γ . As a result, equation (A1) provides a reasonable estimate of the pressure anisotropy required for pitch angle scattering by the ion cyclotron instability to be important on a timescale comparable to the disk rotation period (Ω^{-1}).

If the characteristic timescale for the magnetic field to change by order unity due to turbulence in the accretion disk is Ω^{-1} , then the rate of pitch angle scattering (the ‘‘collision frequency’’) required to ensure that the pressure anisotropy never exceeds the threshold given by equation (A1) is $\nu \delta p \approx \Omega p \rightarrow \nu \approx \Omega \beta_{\parallel,i}^q / S$ where $\delta p = p_\perp - p_\parallel$ is the pressure anisotropy at the threshold in equation (A1). For pitch angle scattering at a rate ν , the ion conductivity is given by

$$\kappa_i \approx \frac{nv_i^2}{\nu} \approx nv_i r \left(\frac{H}{r} \right) \left(\frac{S}{\beta_{\parallel,i}^q} \right) \quad (\text{A2})$$

where the scale-height of the disk is given by $H \approx v_i/\Omega$. Equation (A2) corresponds to $\alpha_c \approx S \beta_{\parallel,i}^{-q} H/r$. Nonlinear simulations of the MRI in RIAFs imply $\beta \sim 10$ in the bulk of the disk, in which case $\alpha_c \approx 0.1H/r$ for the ions. This is, of course, only an upper limit because there may be additional sources of wave-particle scattering and because equation (A2) is the conductivity along field lines while the conductivity used throughout the rest of this paper is an effective isotropic conductivity.

The argument for an upper limit on the electron conductivity proceeds analogously to that above, with equation (A1) being replaced by the corresponding limit on the electron anisotropy induced by the whistler instability. For non-relativistic electrons, Gary & Wang (1996) show that the threshold for the whistler instability is similar to that of equation (A1) with $\beta_{\parallel,i} \rightarrow \beta_{\parallel,e}$. Thus the electron conductivity is given by

$$\kappa_e \approx \frac{nv_e^2}{\nu} \approx nv_e r \left(\frac{H}{r} \right) \left(\frac{S}{\beta_{\parallel,i}^q} \right) \left(\frac{T_i}{T_e} \right)^q \left(\frac{v_c}{v_i} \right). \quad (\text{A3})$$

Equation (A3) is far less restrictive than equation (A2), generally implying $\alpha_c \gtrsim 1$ for the electrons, i.e., no limit on α_c at all (saturation of the electron heat flux, however, implies $\alpha_c \lesssim 1$). This conclusion strictly only applies when the electrons are non-relativistic and more work is needed to understand the extension of this argument to relativistic electrons.

⁴ The mirror instability provides a comparable rate of ion pitch angle scattering (Sharma et al. 2006).

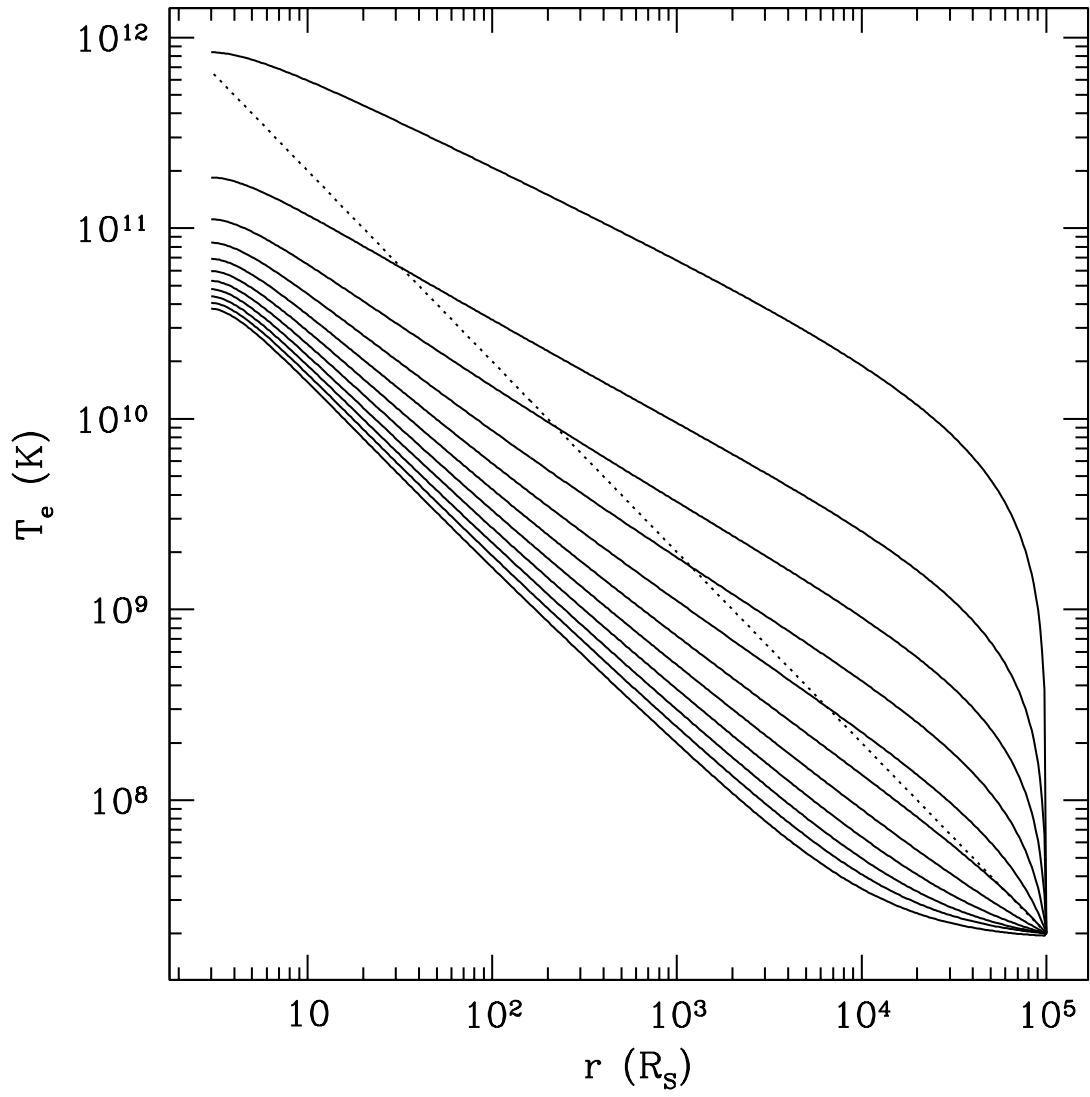


FIG. 1.— Electron temperature for a fixed density profile with $n \propto r^{-p}$, with p varying from 0.5 to 1.5 in increments of 0.1 (from bottom to top). The dotted line is the virial temperature $T_{vir} \propto r^{-1}$. Values for the other parameters are $\alpha_c/\alpha = 1$ and $f_e = 0.1$. For $p \gtrsim 1$, these solutions are unphysical because the electron temperature is super-virial.

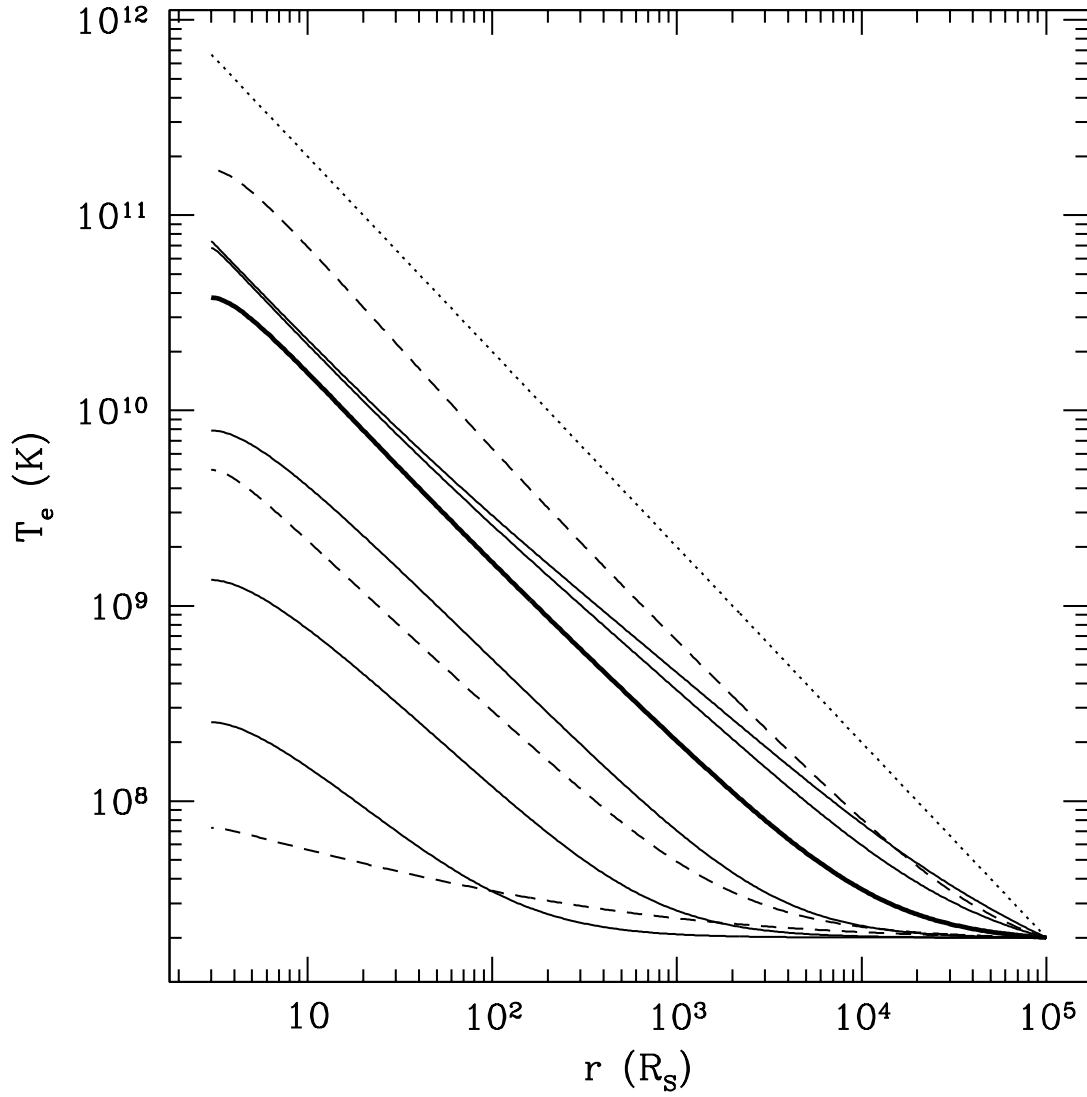


FIG. 2.— Electron temperature with $n \propto r^{-0.5}$ for various α_c/α and f_e . The thick solid line is the calculation from Figure 1 with $p = 0.5$, $\alpha_c/\alpha = 1$ and $f_e = 0.1$. The solid curves correspond to α_c/α varying from 0.01 to 1000 by factors of 10 (from top to bottom). The dashed curves are for $f_e = 0.5$ (top), 0.01 and 0 (bottom). The dotted line is the virial temperature $T_{vir} \propto r^{-1}$. Note that for this density profile the solutions are never super-virial.

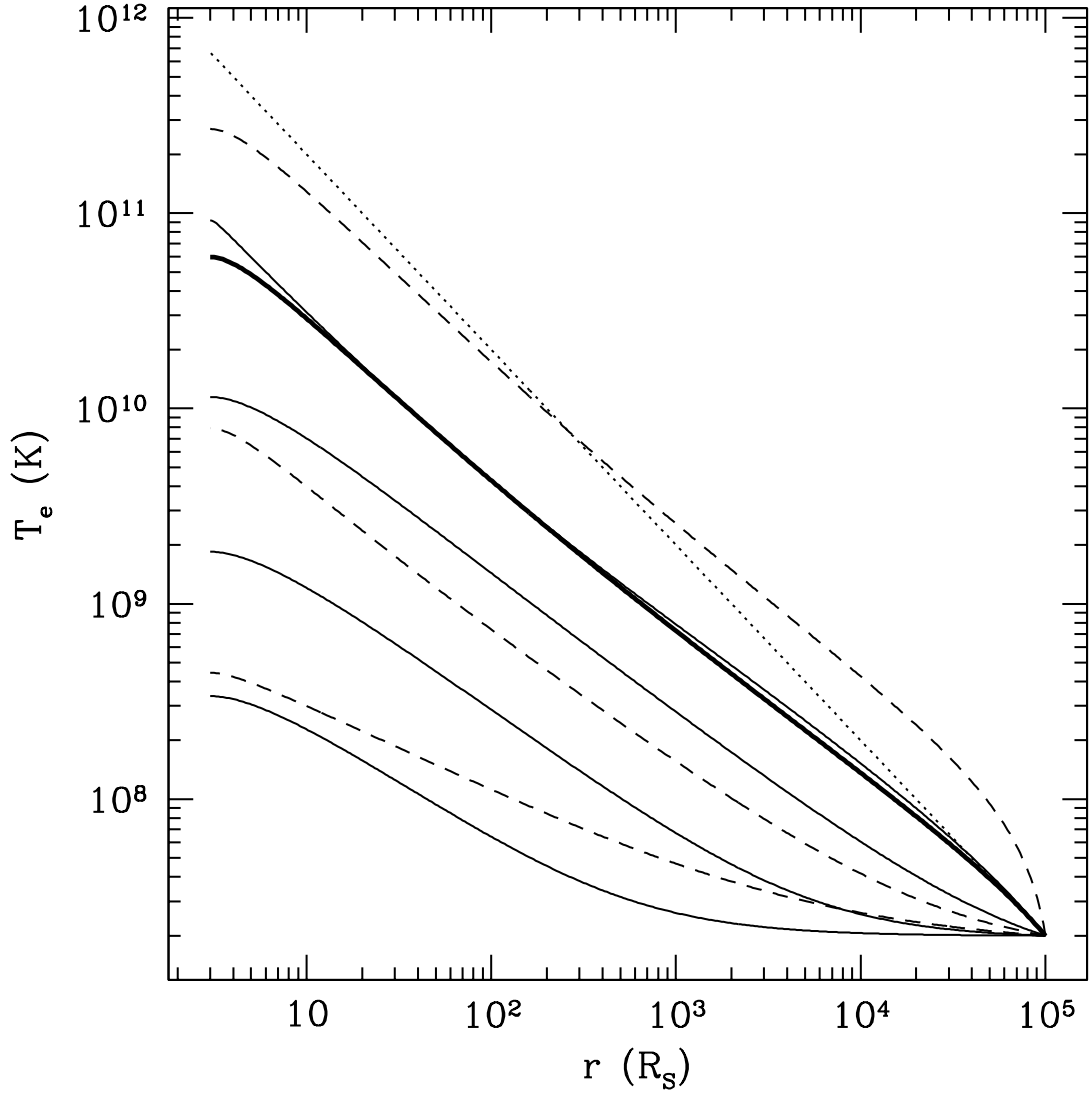


FIG. 3.— Electron temperature with $n \propto r^{-1}$ for various α_c/α and f_e . The thick solid line is the calculation from Figure 1 with $p = 1$, $\alpha_c/\alpha = 1$ and $f_e = 0.1$. The solid curves correspond to α_c/α varying from 0.1 to 1000 by factors of 10 (from top to bottom). The dashed curves are for $f_e = 0.5$ (top), 0.01 and 0 (bottom). The dotted line is the virial temperature $T_{vir} \propto r^{-1}$.

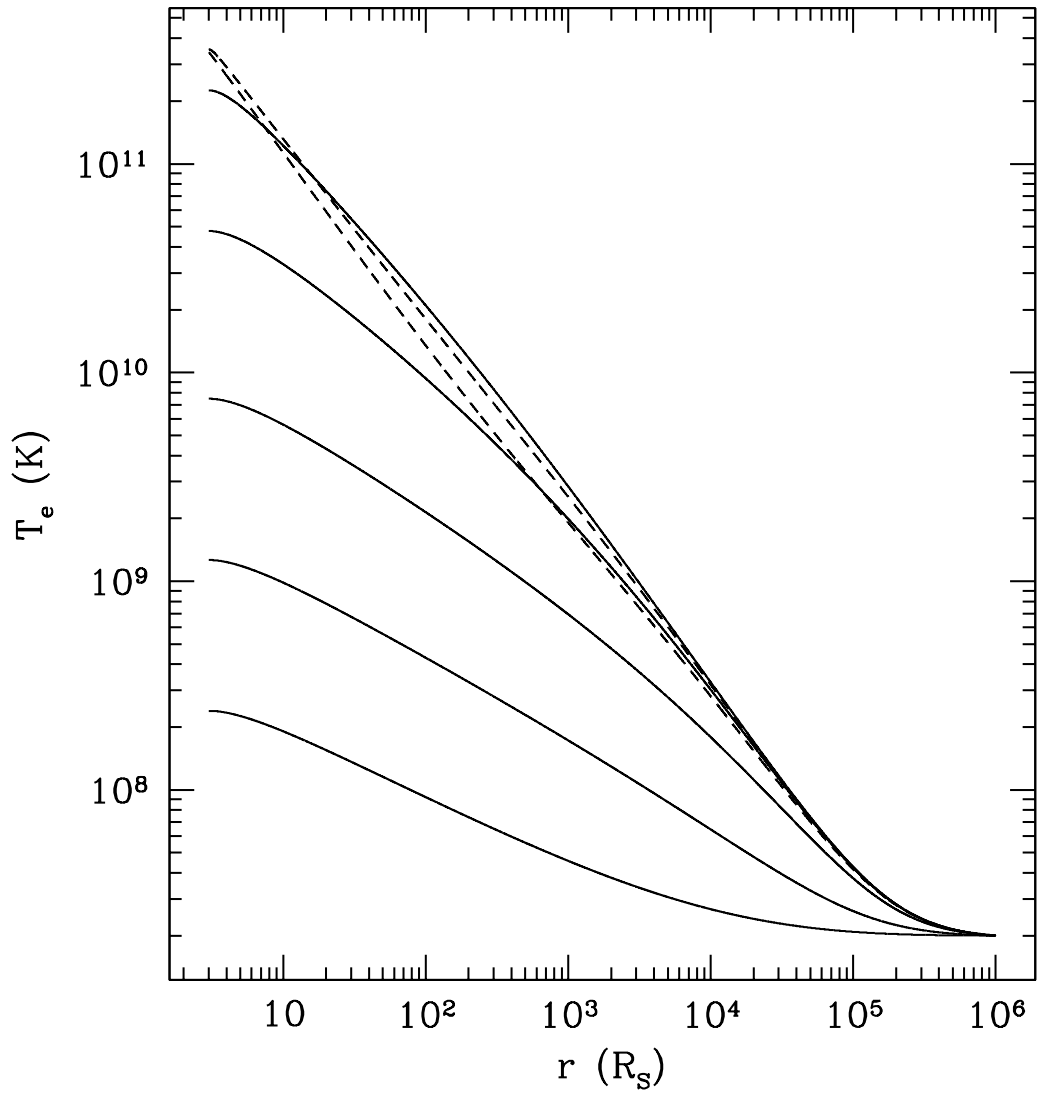


FIG. 4.— Radial temperature profile for the solution of the Bondi accretion problem with heating and conduction, for $f_e = 0.3$. The solid curves correspond to α_c varying from 1 to 10^4 by factors of 10 (from top to bottom). The dashed curves are for $\alpha_c = 10^{-2}$ (top) and 0.1 (bottom).

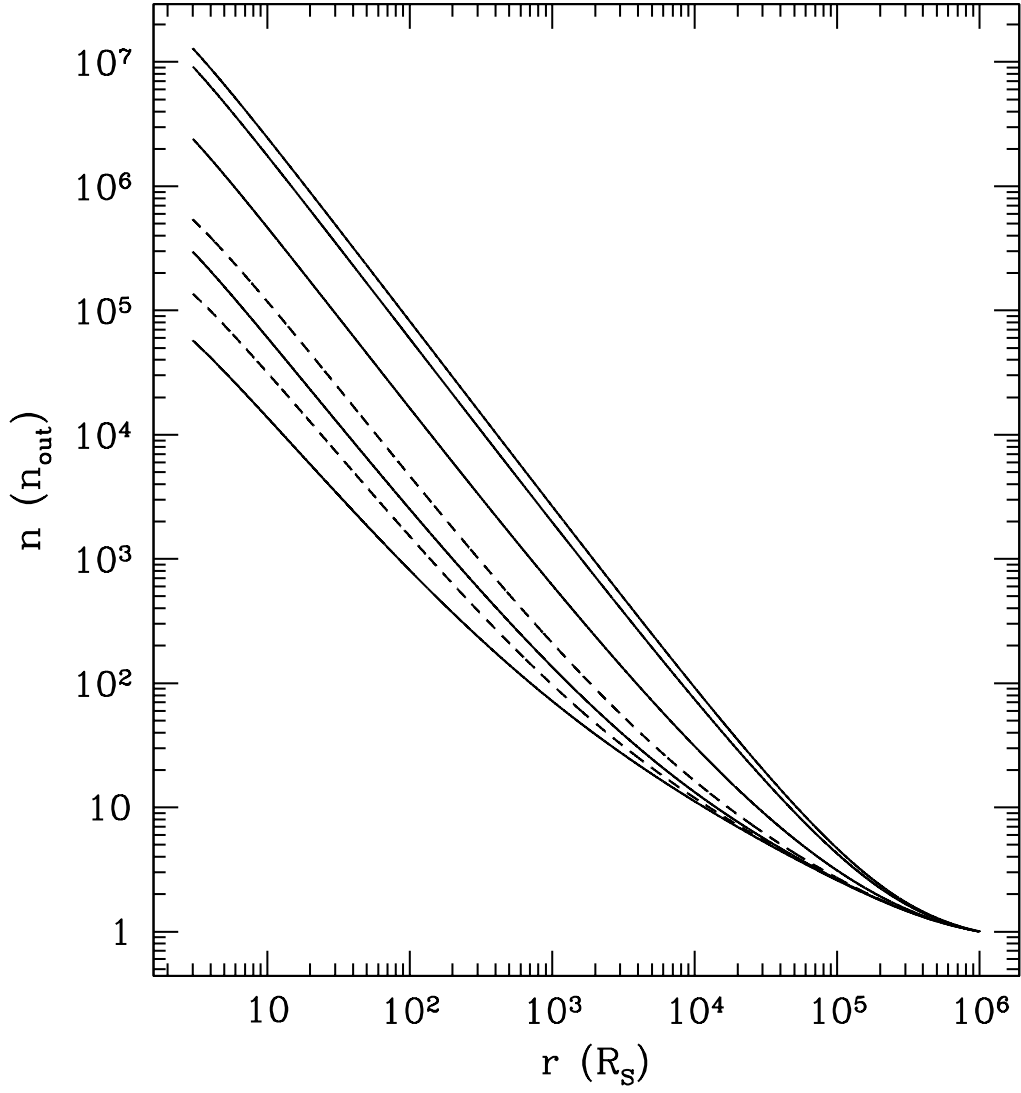


FIG. 5.— Radial density profile for the solution of the Bondi accretion problem with heating and conduction, for $f_e = 0.3$. The solid curves correspond to α_c varying from 1 to 10^4 by factors of 10 (from bottom to top). The dashed curves are for $\alpha_c = 10^{-2}$ (top) and 0.1 (bottom).

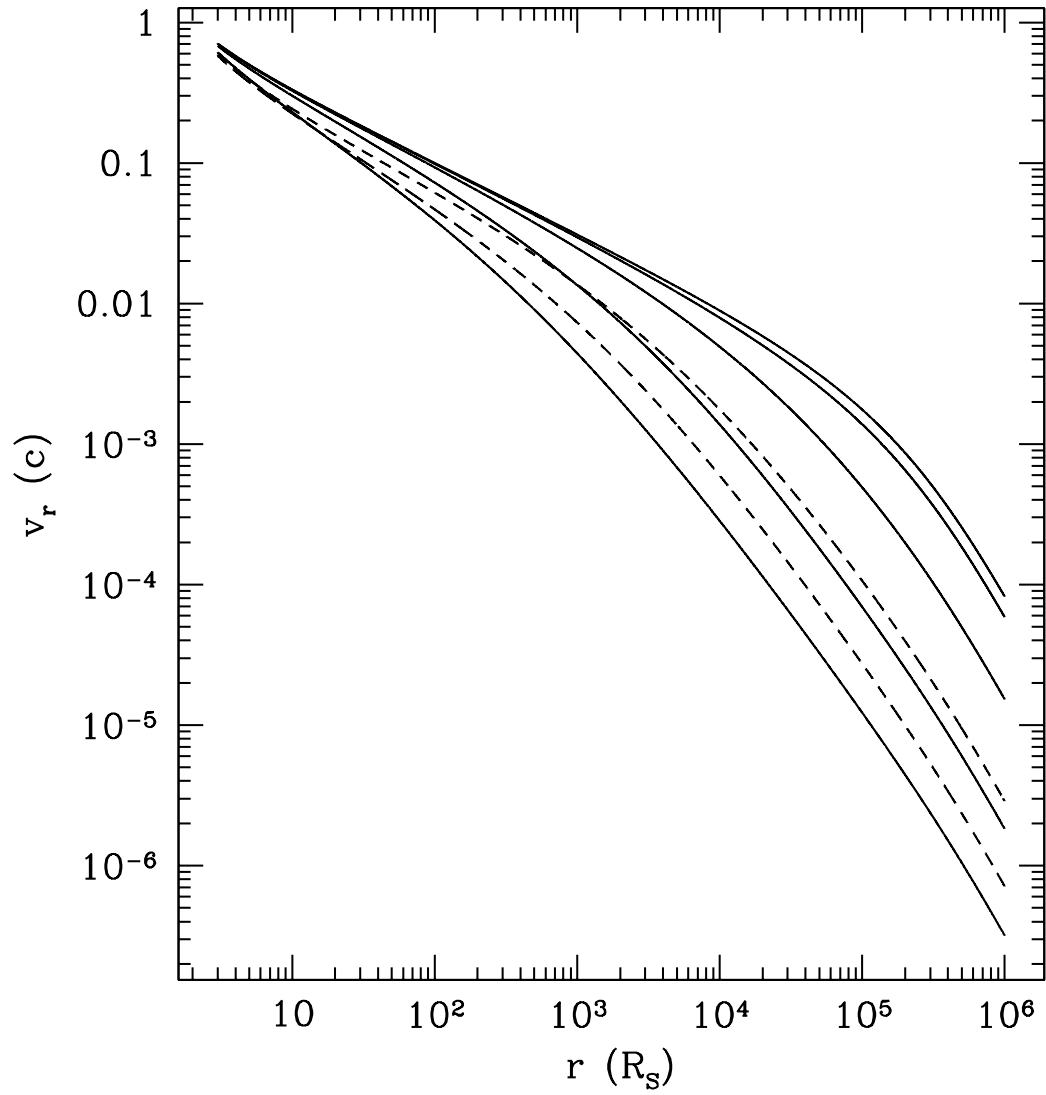


FIG. 6.— Radial velocity profile for the solution of the Bondi accretion problem with heating and conduction, for $f_e = 0.3$. The solid curves correspond to α_c varying from 1 to 10^4 by factors of 10 (from bottom to top). The dashed curves are for $\alpha_c = 10^{-2}$ (top) and 0.1 (bottom).

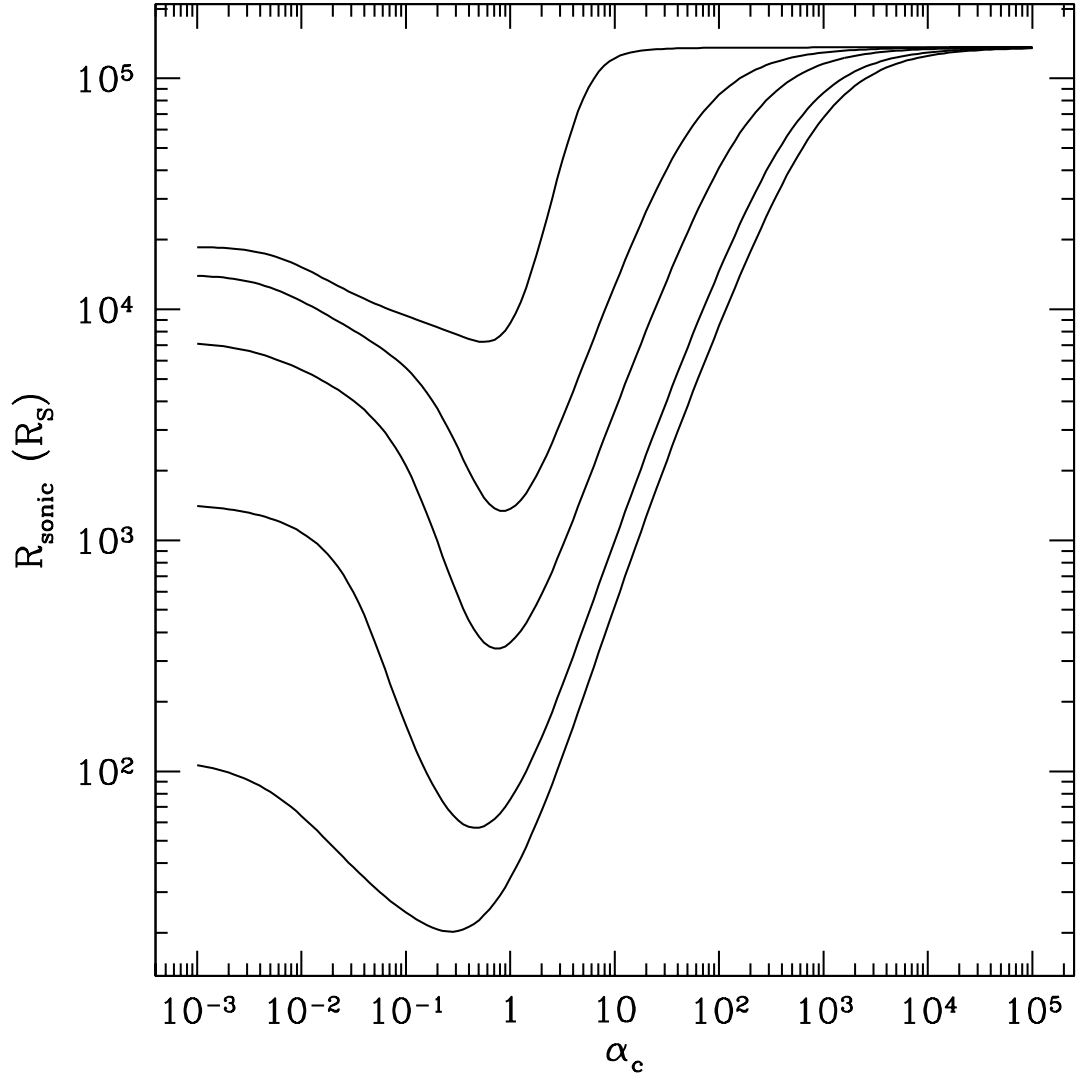


FIG. 7.— Sonic radius (in units of the Schwarzschild radius R_S) as a function of α_c for $f_e = 0$ (top), 0.03, 0.1, 0.3 and 0.5 (bottom).

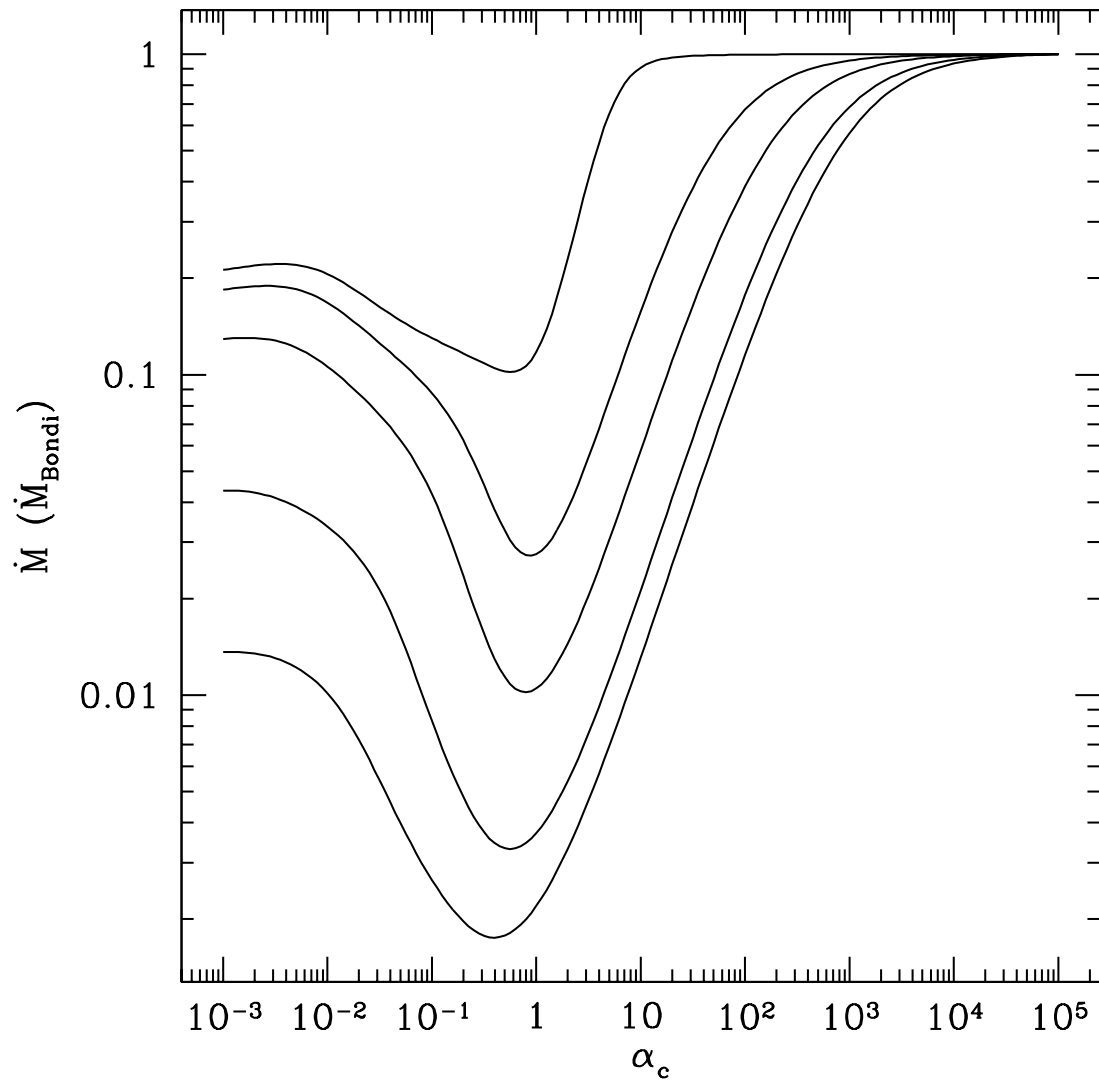


FIG. 8.— Accretion rate (in units of the isothermal Bondi rate) as a function of α_c for $f_e = 0$ (top), 0.03, 0.1, 0.3 and 0.5 (bottom).

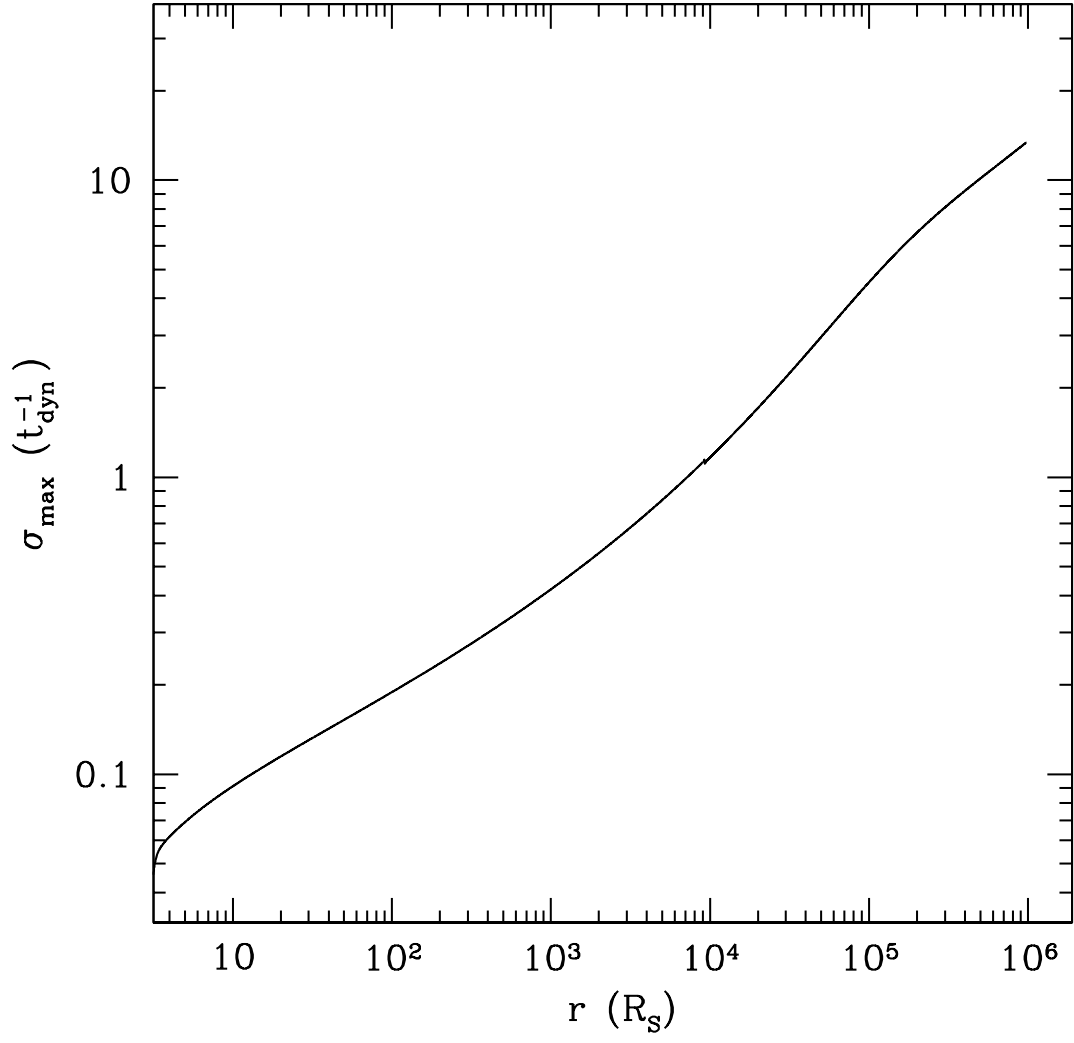


FIG. 9.— MTI growth rate in units of the inverse infall time for a spherical accretion solution from §4; $f_e = 0$ and $\alpha_c = 0.1$. Plotted as a function of radius is the maximum growth rate (equation [29] of Balbus 2000), achieved when the conduction time is short but the tension forces are small.